

Wavelength Dependence of Guiding Properties in Highly Birefringent Elliptical Ring Core Optical Fiber

M. Mazharul Islam¹, M. Anwar Zahid¹, Nazina B. Jamal¹,
M. Rezwana Parvez¹, and M. Shah Alam²

¹Department of Electrical and Electronic Engineering
Military Institute of Science and Technology (MIST)
Mirpur, Dhaka 1230, Bangladesh

²Department of Electrical and Electronic Engineering
Bangladesh University of Engineering and Technology (BUET)
Dhaka 1000, Bangladesh
E-mail: shalam@eee.buet.ac.bd

Abstract—An analysis of highly birefringent optical fiber composed of a central elliptical hollow core with a circular cladding is carried out in this work using finite element method. High birefringence compare to that of the conventional solid elliptical core fiber is obtained. The birefringence properties in terms of various waveguide parameters, e.g., core ellipticity, ratio of hole size and core size, refractive index difference between core and cladding are calculated. The propagation properties, such as, group effective index, group birefringence, and polarization mode dispersion have also been calculated and their wavelength dependence are shown. It can be seen that the dispersion of this hollow core fiber is comparable to that of the conventional polarization maintaining fibers.

Index Terms— Optical fiber, birefringence, finite element method, waveguide, dispersion, refractive index, polarization.

I. INTRODUCTION

IN the past few years, there has been continuous effort to develop highly birefringent (Hi-Bi) optical fibers for single mode operation with high bandwidth [1]-[9]. For this purpose, elliptical core optical fibers are widely used as polarization maintaining fiber (PMF) for many years [4]-[7]. Furthermore, PANDA fibers, bow-tie fibers, side-tunnel fibers are used for this purpose [10]. Recently, fibers with elliptical core having central elliptical air hole are proposed to obtain high birefringence and single polarization with high bandwidth [1]-[6]. High birefringence is obtained with the fiber proposed in [5], and only the birefringence properties with the variations in waveguide parameters are discussed. However, the propagation properties and their wavelength dependence have not been studied in details in [5]. But from application point of view, these studies on propagation properties are essential.

In this work, we have considered the optical fiber of [5], and carried out an analysis using finite element method

(FEM). The results are compared with the results of [5], and good agreement is obtained. Moreover, propagation properties and their wavelength dependence have been studied and shown here. It has been seen that the dispersion limit is comparable to the conventional polarization maintaining fibers.

II. ANALYSIS TECHNIQUE

The optical modal analysis is carried out assuming that the wave propagates along the z -direction and the electric field of the wave has the form

$$\mathbf{E}(x, y, z, t) = \mathbf{E}(x, y) \exp[j(\omega t - \beta z)], \quad (1)$$

where ω is the angular frequency and β is the propagation constant. The fiber guide is assumed to be uniform in the direction of wave propagation. An eigenvalue equation in terms of the electric field can be obtained from the Helmholtz equation

$$\nabla \times (n^{-2} \nabla \times \mathbf{E}) - k_0^2 \mathbf{E} = \mathbf{0}, \quad (2)$$

and is solved for modal effective index, $n_{\text{eff}} = \beta/k_0$, as the eigenvalue. The boundary condition for electric field at the outside of the cladding boundary was set to zero. In the COMSOL Multiphysics [11], however, a module based on the perpendicular hybrid mode wave using transversal fields is used for finding the modal solutions. To do this, the cross sectional domain of the fiber is meshed with the triangular elements while the FEM is used. The birefringence properties and its structural dependence can be obtained easily from the orthogonal mode solutions. The orthogonal modes propagate with different phase velocities and the difference between their effective refractive indices is called the phase birefringence,

$$B = \left| n_e^x - n_e^y \right|. \quad (3)$$

If light is injected into the fiber so that both the orthogonal modes are excited, then one will be delayed in phase relative to the other as they propagate. When this phase difference is an integral multiple of 2π , the two modes will beat at this point and the input polarization state will be reproduced [10]. The length over which this beating occurs is the fiber beat length,

$$L_B = \frac{\lambda_0}{B}, \quad (4)$$

where λ_0 is called the free-space wavelength.

III. WAVELENGTH DEPENDENT GUIDING PROPERTIES

To find the wavelength dependent guiding properties, the following Sellmeier equation is used to obtain wavelength dependent refractive indices [10]:

$$n^2 - 1 = \frac{A_1 \lambda^2}{(\lambda^2 - \lambda_1^2)} + \frac{A_2 \lambda^2}{(\lambda^2 - \lambda_2^2)} + \frac{A_3 \lambda^2}{(\lambda^2 - \lambda_3^2)}, \quad (5)$$

where SiO_2 is used as cladding material and $\text{GeO}_2:\text{SiO}_2$ as core material. The constants of (5) for cladding material are taken from [10] as, $A_1=0.6961663$, $A_2=0.4079426$, $A_3=0.8974794$, $\lambda_1=0.0684043$, $\lambda_2=0.1162414$, $\lambda_3=9.896161$ and those for core material are $A_1=0.711040$, $A_2=0.451885$, $A_3=0.704048$, $\lambda_1=0.064270$, $\lambda_2=0.129408$, $\lambda_3=9.425478$. Now, to obtain wavelength dependent properties, for each wavelength the optical analysis has to be carried out with the corresponding refractive index of core and cladding. Once the effective index versus wavelength curve is obtained, one can obtain the group index for the orthogonal polarizations using

$$N_e = n_e - \lambda \frac{dn_e}{d\lambda}, \quad (6)$$

where N_e is the group effective index of desired polarization at an wavelength, λ . Now, it is possible to obtain group birefringence from the group effective indices. Then one can express the group birefringence as

$$B_g = \left| B - \lambda \frac{dB}{d\lambda} \right|. \quad (7)$$

The total dispersion is the total effect of material and waveguide dispersion. It is calculated in a similar way as for calculating waveguide dispersion. In this case the fiber refractive index profile depends on wavelength. The material dispersion effect should be calculated first. Then the mode effective index n_{eff} is calculated by the mode solver [11].

The total dispersion of a fiber can be calculated as

$$D_{total} = -\frac{\lambda}{c} \frac{d^2 n_{eff}}{d\lambda^2}. \quad (8)$$

The polarization mode dispersion (PMD) on the other hand may be calculated at this stage of analysis. The PMD is known to be proportional to group delay [10]. So, in terms of group delay, it can be expressed as

$$\tau = \frac{1}{c} \left(B - \lambda \frac{dB}{d\lambda} \right) = \frac{B_g}{c}, \quad (9)$$

where c is the velocity of light. So, the PMD can be evaluated on the basis of group birefringence. In the following section, we show different propagation properties on the basis of the discussion of this section and the previous section.

IV. RESULTS AND DISCUSSION

The cross section of the elliptical hollow core optical fiber is shown in Fig. 1. For the fiber, the elliptical air hole is concentric with the elliptical ring core and the

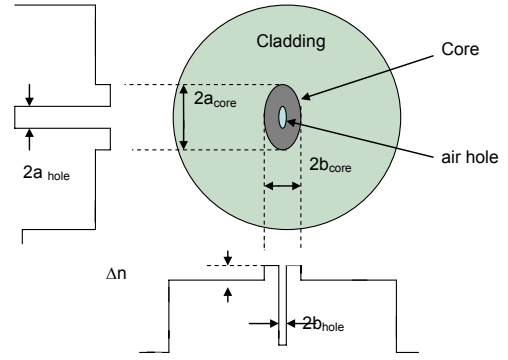


Fig. 1. The cross section of the elliptical ring core optical fiber [5].

key waveguide parameters are the major and the minor axes of the air hole and the ring core, a_{hole} , a_{core} , b_{hole} , and b_{core} , respectively, and the refractive index difference between the core and cladding, Δn . To show the validity of our approach, we first compare our results with those of [5] in Fig. 2, where birefringence versus normalized frequency, V_{ab} is shown. The normalized frequency, V_{ab} is defined as [5]

$$V_{ab} = \frac{2\pi \sqrt{(a_{core} b_{core})}}{\lambda} \sqrt{n_{core}^2 - n_{clad}^2} = \frac{2\pi a_{core} \sqrt{(n_{cladding} \Delta n)}}{\lambda},$$

where $b_{core}/a_{core}=0.5$ is taken. The hole size is represented as a ratio of the core size defined by a_{hole}/a_{core} . In Fig. 2, the solid lines show our results and dark circles show the results of Hwang et. al. [5]. For $\Delta n=0.02$, both the results agreed well, but for $\Delta n=0.01$, a slight difference can be seen, which may be due to the use of different method or insufficient number of elements in the solution domain when FEM is used in our analysis. As was explained in [5], a maximum birefringence can be obtained at a normalized frequency $V_{ab}=2$ when $\Delta n=0.02$.

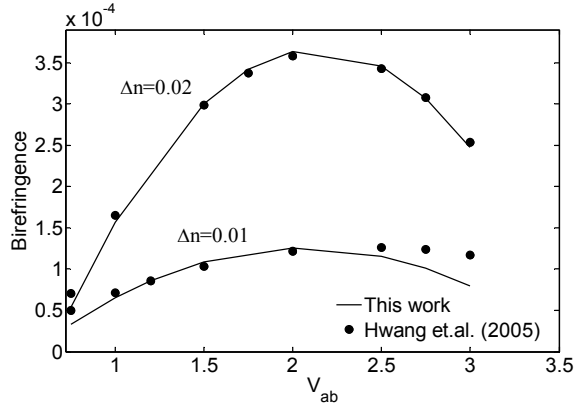


Fig. 2. Birefringence versus normalized frequency.

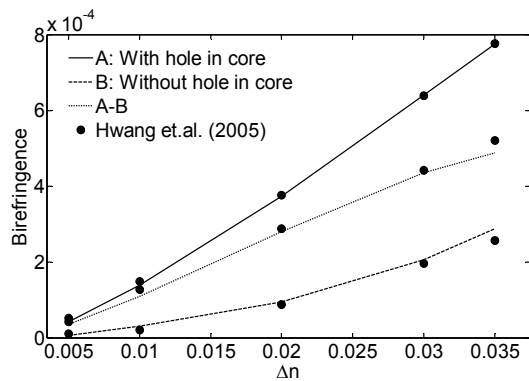
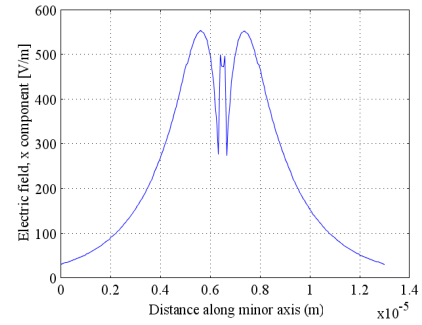
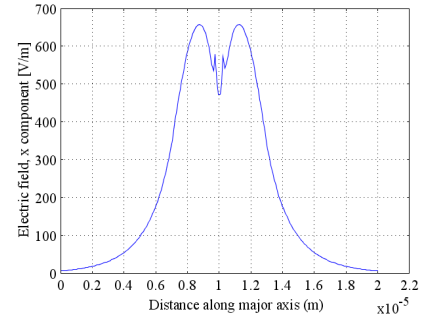


Fig. 3. Birefringence versus the difference of index between core and cladding, Δn .

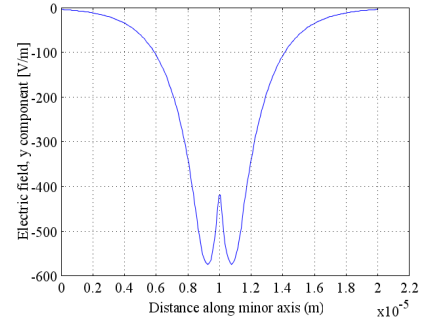
Fig. 3 shows the birefringence versus the difference of index between core and cladding, Δn . We have again compared our results with those of Hwang et. al. [5]. The dark circles show the results of [5] and a very good agreement can be seen in this figure. Thus, our analysis using FEM is verified. This figure shows the birefringence maxima achievable with each Δn , here the solid line A is the maxima of the total birefringence when there is hole in the core, the large dashed line B is for the birefringence when $a_{\text{hole}}=0$, that means without hole in core, and the small dashed line shows the difference in birefringence, A-B, of the other two shown by solid line and the large dashed line; this difference is obviously the birefringence due to the core and air hole boundary effect. The electric field intensity distribution is shown in Fig. 4. The core-cladding index difference was set to be 0.02 and the operating wavelength is $1.55\mu\text{m}$. One can see significantly different field distributions around the air hole for two orthogonal polarizations. For x-polarization, the electric field is discontinuous at the air-core interface on both the major and minor axes and there is a prominent depression of intensity on minor axis. For y-polarization, the electric field is continuous at the air-core interface on minor axis but discontinuous on major axis and a depression of intensity can be seen there. These are also discussed in a similar way in [5].



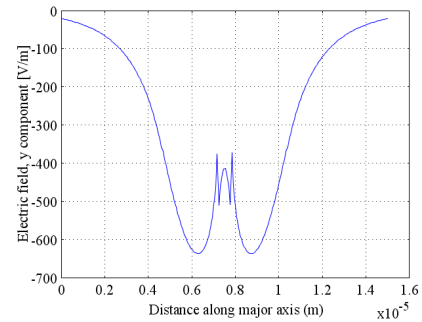
(a)



(b)

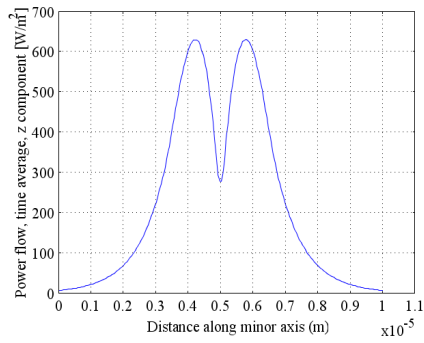


(c)

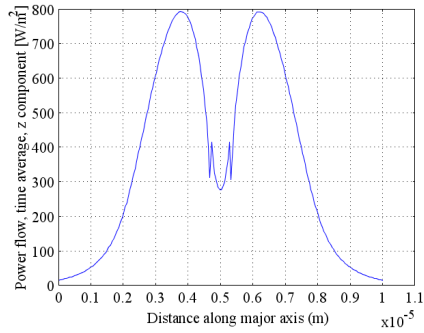


(d)

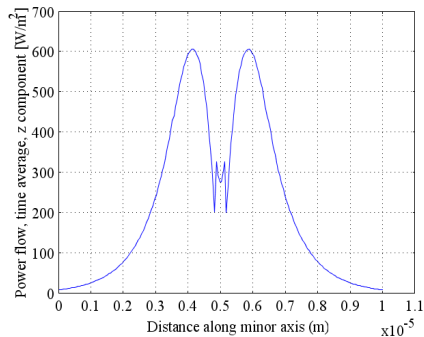
Fig. 4. The electric field intensity distribution, (a) along minor axis for x-polarization, (b) along major axis for x-polarization, (c) along minor axis for y-polarization, (d) along major axis for y-polarization mode.



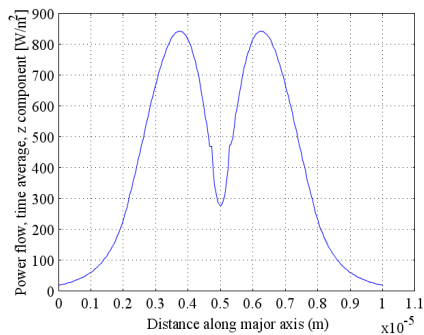
(a)



(b)



(c)



(d)

Fig. 5. The power distribution, (a) along the length of minor axis for y -polarization, (b) along the length of major axis for y -polarization, (c) along the length of minor axis for x -polarization, (d) along the length of major axis for x -polarization.

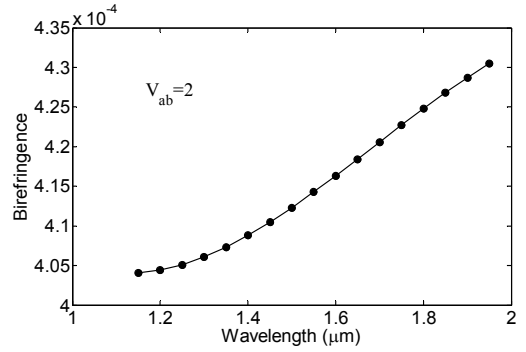


Fig. 6. The birefringence versus wavelength.

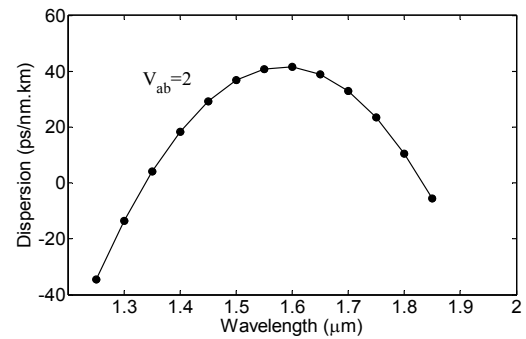


Fig. 7. Group velocity dispersion versus wavelength.

Fig. 5 shows propagating power distribution of the field in the fiber along the major and minor axes of the core for x - and y -polarizations. This study can be helpful for the understanding of the beam shape and splicing performance of the fiber. Discontinuities are there at the air-core interfaces on major axis for y -polarization and on minor axis for x -polarization. These are due to the field discontinuities at the respective interfaces. The overall power distribution in this case takes an annular shape with slightly squeezed along minor axis. For conventional fibers, the power distribution is typically have a Gaussian shape, but in this case it shows a dip in the center, which expands only over a very narrow region of central air hole, thus, a Gaussian shape may be presumed.

Next, wavelength versus birefringence is shown in Fig. 6 at normalized frequency $V_{ab}=2$. With the increase in wavelength, the birefringence increases. At $1.55\mu\text{m}$, it is about 4.13×10^{-4} . The birefringence value is in the order of 10^{-4} in the wavelength region considered in this work. This is sufficiently high compared to other solid core PMFs. Fig. 7 shows the group velocity dispersion versus wavelength. Zero-dispersion occurs at wavelengths near $1.35\mu\text{m}$ and $1.84\mu\text{m}$ and maximum dispersion occurs at $1.60\mu\text{m}$. However, the dispersion level is comparable to conventional optical fibers.

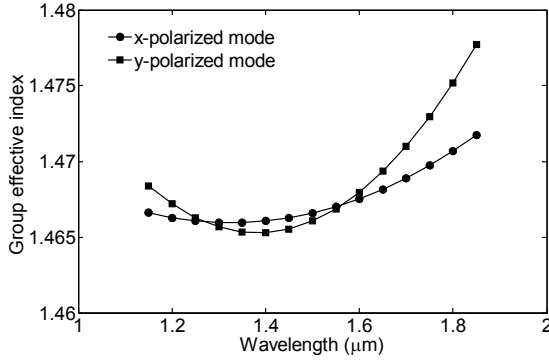


Fig. 8. The group effective index versus wavelength.

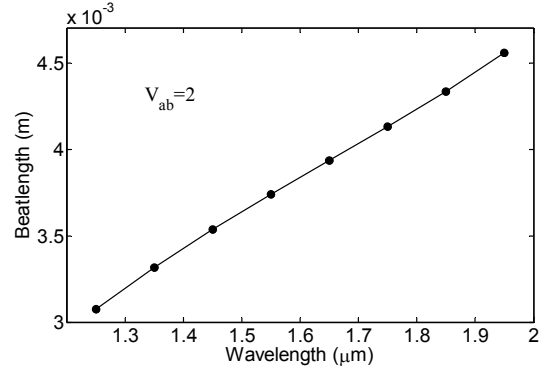


Fig. 10. The beat length versus wavelength.

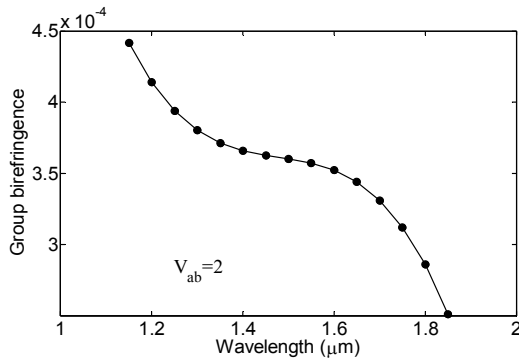


Fig. 9. The group birefringence versus wavelength.

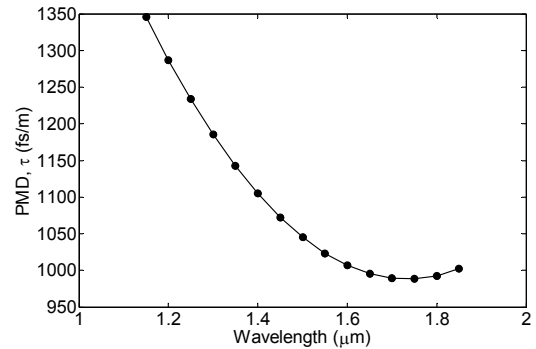


Fig. 11. Polarization mode dispersion versus wavelength.

Fig. 8 shows the group effective index versus the wavelength for x and y -polarized modes. The pattern is very similar to conventional step index fibers and over a range of about $20 \mu\text{m}$ of wavelength, the group effective index does not change rapidly. The group birefringence versus wavelength is shown in Fig. 9. Though the phase birefringence increases with the increase in wavelength, the group birefringence decreases with the increase in wavelength. But, the order of magnitude remains unchanged at 10^{-4} . Next, in Fig. 10, we show the beat length property of the fiber. Beat length increases with the increase in wavelength. Finally, Fig. 11 shows the polarization mode dispersion of the fiber. This is expressed in terms of the differential group delay per unit length of the fiber and is found to be decreasing with the increase in wavelength.

V. CONCLUSION

An analysis of highly birefringent optical fiber composed of a central elliptical hollow core with a circular cladding is carried out in this work using finite element method. High birefringence compare to that of the conventional solid elliptical core fiber is obtained. The birefringence properties

in terms of various waveguide parameters, e.g., ellipticity, ratio of hole size and core size, refractive index difference between core and cladding are calculated. The propagation properties, such as, group effective index, group birefringence and dispersion have also been calculated and their wavelength dependence are shown. It can be seen that the dispersion limit is comparable to the conventional polarization maintaining fibers.

REFERENCES

- [1] S. Choi, K. Oh, W. Shin, C. S. Park, U. C. Paek, K. J. Park, Y. C. Chung, G. Y. Kim, and Y. G. Lee, "Novel Mode Converter Based on Hollow Optical Fiber for Gigabit LAN Communication," *IEEE Photon. Technol. Lett.*, vol. 14, no. 2, pp. 248-250, Feb. 2002.
- [2] S. Choi, T. J. Eom, J. W. Yu, B. H. Lee, and K. Oh, "Novel all-fiber bandpass filter based on hollow optical fiber," *IEEE Photon. Technol. Lett.*, vol. 14, no. 12, pp. 1701-1703, Dec. 2002.
- [3] K. Oh, S. Choi, Y. Jung, and J. W. Lee, "Novel Hollow Optical Fibers and Their Applications in Photonic Devices for Optical Communications," *IEEE J. Lightwave Technol.*, vol. 23, no. 2, pp. 524-532, Feb. 2005.

- [4] Y. Jung, S. R. Han, S. Kim, U. C. Paek, and K. Oh, "Versatile control of geometric birefringence in elliptical hollow optical fiber," *Optics Lett.*, vol. 31, no. 18, pp. 2681-2683, Sept. 2006.
- [5] I. -K. Hwang, Y. -H. Lee, K. Oh, and D. N. Payne, "High birefringence in elliptical hollow optical fiber," *Optics Express*, vol. 12, no. 9, pp. 1916-1923, May 2004.
- [6] M. -J. Li, X. Chen, D. A. Nolan, G. E. Berkey, J. Wang, W. A. Wood, and L. A. Zenteno, "High Bandwidth Single Polarization Fiber With Elliptical Central Air Hole," *IEEE J. Lightwave Technol.*, vol. 23, no. 11, pp. 3454-3460, Nov. 2005.
- [7] D. A. Nolan, G. E. Berkey, M. -J. Li, X. Chen, W. A. Wood, and L. A. Zenteno, "Single-polarization fiber with a high extinction ratio," *Optics Lett.*, vol. 29, no. 16, pp. 1855-1857, Aug. 2004.
- [8] W. Xue, G. Zhou, Y. Xiao, and R. Yang, "Analysis of Dispersion Properties in Hexagonal Hollow Fiber," *IEEE J. Lightwave Technol.*, vol. 22, no. 8, pp. 1909-1914, Aug. 2004.
- [9] X. Chen, M. -J. Li, J. Koh, and D. A. Nolan, "Wide band single polarization and polarization maintaining fibers using stress rods and air holes," *Optics Express*, vol. 16, no. 16, pp. 12060-12068, July 2008.
- [10] G. P. Agrawal, "Nonlinear Fiber Optics," 3rd Edition, Elsevier, 2006.
- [11] COMSOL Multiphysics, version 3.2, Sept. 2005.
- [12] H. Shu and M. Bass, "Calculating the Guided Modes in Optical Fibers and Waveguides," *IEEE J. Lightwave Technol.*, vol. 25, no. 9, pp. 2693-2699, Sept. 2007.
- [13] Y. Zhu, X. Chen, Y. Xu, and Y. Xia, "Propagation Properties of Single-Mode Liquid-Core Optical Fibers With Subwavelength Diameter," *IEEE J. Lightwave Technol.*, vol. 25, no. 10, pp. 3051-3056, Oct. 2007.
- [14] E. M. Dianov and V. M. Mashinsky, "Germania-Based Core Fibers," *IEEE J. Lightwave Technol.*, vol. 23, no. 11, pp. 3500-3508, Nov. 2005.
- [15] K. Saitoh, S. K. Varshney, and M. Koshiba, "Dispersion, birefringence, and amplification characteristics of newly designed dispersion compensating hole-assisted fibers," *Optics Express*, vol. 15, no. 26, pp. 17724-17734, Dec. 2007.